JOURNAL OF NEUROTRAUMA
Volume 24, Number 5, 2007

Pp. 885–894
DOI: 10.1089/neu.2006.0156

Aging Delays the Regeneration Process following Sciatic Nerve Injury in Rats

***YONG-JUN WANG,[1,2] *CHONG-JIAN ZHOU,[1,2] QI SHI,[1,2] NATHAN SMITH,[3] and TIAN-FANG LI[4]**

ABSTRACT

The present study investigated the effect of aging on muscle reinnervation in rats following a crush nerve injury. Using confocal laser scanning microscopy, we examined the spatial correlation of terminal Schwann cells (TSCs) or axon terminals with acetylcholine receptor (AChR) sites at neuromuscular junctions (NMJs). Compared to young rats (4 months of age), aged rats (24 months of age) demonstrated damaged TSC extensions and delayed regeneration. Post-injury endplate abnormalities in aged rats correlated with the degree of TSC degeneration. In the late stages of reinnervation, pathologic changes were seen in old rats, including multiple innervations, terminal sprouting, and poorly formed collateral innervation in NMJs. Our results suggest that the impaired TSC-axon interaction in aged rats delays the reinnervation process.

Key words: aging; confocal microscopy; immunohistochemistry; nerve regeneration; neuromuscular junctions; protein-gene-product 9.5; Schwann cell

INTRODUCTION

SCHWANN CELLS (SCs) promote neurite growth and regulate local intercellular actions involved in extension and directional guidance of axons during muscle reinnervation following injury (Son et al., 1995a). In both developing and regenerating neuromuscular junctions (NMJs), robust proliferation of SCs is seen as the NMJ matures (Love et al., 1998). However, partial denervation of a skeletal muscle is followed by the growth of fine processes (sprouts) from the remaining intramuscular nerve fibers, eventually leading to reinnervation of denervated muscle fibers (Brown et al., 1981). These sprouts may arise either from unmyelinated pre-terminal segments of the axon (terminal sprouting) or from nodes of Ranvier (nodal or collateral sprouting) (Zhou et al., 2002).

Previous studies have shown that age affects the regenerative capability of peripheral nerve fibers. In older rats, regeneration of the axontomized peripheral nerve is delayed because of lower numbers of regenerating axons and sprouts; NMJ reinnervation is also delayed (McMartin et al., 1979; McQuarrie et al., 1989; Tanaka et al., 1991; Vaughan et al., 1992; Hopkins et al., 1986; Acob et al., 1990). To date, the SC-axon interactions in the motor endplate region of aging mammals has not been investigated.

In this study, we studied the effect of age on the process of axonal outgrowth. Morphological changes of the ter-

[1]Institute of Spine and [2]Longhua Hospital, Shanghai University of Traditional Chinese Medicine, Shanghai, China.
[3]Center of Aging and Development and Department of Neurosurgery, and [4]Center for Musculoskeletal Research, University of Rochester, Rochester, New York.
*Both authors contributed equally to this work.

minal Schwann cells (TSCs), axon terminals, and postsynaptic acetylcholine receptor (AChR) sites were examined following a crush injury of the sciatic nerve. The following markers were used: the protein gene product 9.5 (PGP 9.5) for axon, S100 for TSC, and C-bungarotoxin (C-BT) for AChR. After labeling, the samples were analyzed with a three-dimensional imaging system. Our results demonstrate specific age-related changes in TSCs and AChR sites.

METHODS

Animal Surgery

Two groups of male Wistar rats were utilized: 30 young adults (4 months old, weight 315 ± 19 g), and 38 aged rats (24 months old, 535 ± 55 g). Animals were deeply anesthetized with ether, followed by subcutaneous injection of sodium pentobabiturate (50 mg/kg). The right sciatic nerve was exposed and crushed for 30 sec with microforceps until a 2-mm translucent portion was created. The skin was sutured closed, and the animals were monitored for recovery from anesthesia and then returned to their usual habitat. All surgical procedures were approved by the Ethical Committee for Animal Management in Shanghai University of Traditional Chinese Medicine.

Tissue Samples

The soleus muscles and sciatic nerves from five young and aged rats were examined at 1, 4, 8, and 12 weeks post-crush (WPC). Unoperated rats were used as controls. Following euthanasia, the animals were perfused with 10mM phosphate-buffered saline (PBS, pH 7.6), followed by 300 mL of fixative (4% paraformaldehyde in 0.1M phosphate buffer, pH 7.4). The soleus muscles were removed and post-fixed for 8 h. After incubation in serial sucrose solutions, the samples were frozen in isopentane pre-cooled by dry ice and stored at −80°C until use. For better antigen detection, free-floating sections were used.

Longitudinal sections (50 μm) were cut on a freezing microtome (Frigocut, Germany) at −20°C and were collected in PBS. The sections were taken exclusively from the middle core of the muscle, where the nerve bundles and nerve terminals cross the long axis of the muscle.The crushed sciatic nerve samples were fixed, dehydrated, cleared and embedded. At least four consecutive sections (7 μm) were obtained from the sagittal plane and stained using hematoxylin and eosin (H&E). Morphometric analysis was performed using an image auto-analysis system (CMIAS-99B, Italy).

Immunohistochemistry

The sections were rinsed with PBS followed by 0.4% Triton-X 100. Non-specific binding sites were blocked by pre-incubation with 1% bovine serum albumin (BSA) in PBS supplemented with 0.05% NaN3 for 1 h at room temperature (RT). The sections were then incubated with the following primary antibodies overnight at RT: anti-protein gene product 9.5 (PGP 9.5, a neuron-specific protein found in neuronal cell bodies and axons, diluted 1:2000; Ultraclone, Cambridge, UK); anti-S100 (a marker for TSCs, diluted 1:40; Nichirei, Tokyo, Japan). Non-immune rabbit serum (1:400) was used as negative control. After washes, appropriate secondary antibody (goat anti-rabbit IgG, 1:200; Vector Laboratories, Burlingame, CA) was applied onto the sections and incubated at RT for 4 h. After rinsing, the sections were then incubated with streptavidin labeled with Texas red (1:200; Vector) for 2 h. The stained sections were placed on slides pretreated with 0.1% poly-L-lysine (Sigma, St. Louis, MO) to prevent shrinkage. Labeling of the postsynaptic acetylcholine receptor (AChR) site was achieved by incubation with FITC-conjugated C-bungarotoxin (C-BT, 1:50; Molecular Probes, Eugene, OR). Slides were finally washed and mounted with Vectashield (Vector).

Confocal Laser Scanning Microscopy

The sections double-labeled with FITC and Texas red were scanned using excitation at 488 nm (argon laser, for FITC) and 568 nm (krypton laser, for Texas red) with a confocal laser scanning microscopy system (CLSM-GB 200 Olympus, Japan). Serial optical sections were transferred to separate channels in order to avoid interference and then superimposed. Optical sections at intervals of 0.5–1 μm were projected on a single plane extending 10–40 μm in thickness and re-constructed to show superimposed images of either the TSC/AChR sites or the axon terminals/AChR sites.

Morphometric Analysis

For quantitative analysis of the reconstructed three-dimensioned images, several sections were selected from each rat. Power analysis determined that at least 15 NMJs per section, with a minimum of five sections per rat, were required for statistical reliability. Only motor endplates cut in the tangential plane were selected. The area of the motor endplate was defined as the sites where pre-terminal SCs or axon terminal met the C-BT positive AChR. One motor endplate was often organized into two or more groups, each of which contained a collection of terminal SCs or nerve terminal branches. To avoid errors in statistical analysis, we excluded motor endplates with un-

defined borders. In the regions with superimposition of presynaptic elements and postsynaptic receptors, merging of Texas red-labeled S100 or PGP9.5 with FITC-labeled α-BT produced a yellow color. The dual-colored images were digitally converted to grayscale. The nonoverlapped areas from presynaptic and postsynaptic elements were then removed by digital subtraction. Selected superimposed areas were measured. To minimize the subjective bias in delineation of the borders of the structure, the scope of the gray image was always compared with both the original color image as well as normal controls. The analysis was performed independently by two investigators.

Statistical Analysis

One-way ANOVA was used to analyze the values of the samples obtained at different time points.

RESULTS

Using a double fluorescence technique, longitudinal sections of the soleus were labeled with S-100 and C-BT, at the region of the NMJ. The reconstructed three-dimensioned images show that in young unoperated control samples complete and accurate spatial occupancy is observed between TSCs and postsynaptic receptor regions and that the ring-shaped AChR plaques are uniformly distributed throughout the muscle, a phenomenon not seen in aged controls. At 1-WPC, young rats demonstrate robust TSC extensions, some of which overlap with AChR sites. Degenerative changes, characteristic of shrinkage and fragmentation, are found in AChR sites. The nerve bundles and their extensions from TSCs are sparser in the aged rats.

By 4-WPC, single or multiple TSCs extend over the NMJ in young animals; however, the engagement is incomplete, as indicated by a large area of AChR plaques compared to the TSC extensions. The ongoing regeneration process was indicated by round or oval TSCs with well-defined margins overlapping AChR plaques. While a similar process occurs in aged animals, there is less organization, with a lack of spatial co-ordination between TSCs and AChRs; many AChR sites have no overlapping TSC extensions. By 8-WPC, older rats showed S-100 labeling of the AChR by round- or spindle-shaped TSC extensions identical to that of TSCs in young rats. Unique loop-like debris, composed of TSC and AChR, is seen. The majority of the NMJs demonstrate complete superposition with the TSC extensions formed in response to the injury at 12-WPC. The S-100 labeled cell strands were generally sparse, with poorly formed thin processes extending from the cell body contacting the underlying AChR plaque in most of the NMJs. Besides the large portions of the AChR geometry which TSCs failed to occupy at 8-WPC, the S-100 immunostaining in aged animals displayed degeneration profiles of the SC strands and TSCs up to 12-WPC. The overall picture in aged rats is one of less developed TSCs coupled with poorly developed AChR plaques, which is infrequently found in young rats. The SC strands displayed either misaligned, disordered bundles or poor development (Figs. 1 and 2).

We then carried out double fluorescence labeling of PGP9.5 and C-BT on soleus samples of both young and aged rats (Figs. 3 and 4). In young, unoperated controls, complete and accurate spatial occupancy between nerve terminals and postsynaptic receptor regions was seen. On the contrary, marked complexity in apposition between the nerve terminal and postsynaptic receptor sites was observed in aged junctions. At 1-WPC in young and aged rats, the axon terminals are disorganized and disintegrated in most NMJs. However, the nerve bundles were sparse and there were fewer axon terminals in NMJs in aged rats. In young animals at 4-WPC, multiple PGP9.5-labeled extensions from nerve trunks entered the NMJs. Some NMJs were reinnervated by a process of sprouting, and the major source of reinnervation was extraterminal sprouting developing into endplate-to-endplate connections. By 8-WPC, the extensions from nodal sprouting resulted in multiple innervations of the same NMJ. Well-organized terminal axons gradually became common, followed by mixed nodal and extraterminal sprouting. At 12-WPC, much of the postsynaptic receptor region in young rats became covered by well-defined elaborate arborizations (Fig. 3).

In aged rats at 4-WPC, postsynaptic receptor regions were markedly disorganized. Although the distal extensions traced to NMJs, the terminal expansions were poorly formed, and there was poor development of the endplate-to-endplate connections. By 8-WPC, the shrinkage of the postsynaptic receptor regions was persistent. Randomly aligned preterminal extensions and persistent poorly-developed nerve terminals were shown. Histologic features of preterminal extensions from aged NMJs include the following: (1) meandering preterminal extension and extensive tangles of unfasciculated thin and/or thick extensions clumping near NMJs or around the nerve bundles; (2) tortuous endplate-to-endplate connections and disordered developing terminals; (3) several NMJs lying close to each other, each supplied by a short branch coming from one of the randomly aligned preterminal extensions (Fig. 4).

To quantitatively analyze the differences demonstrated between the young and aged groups, we measured the extent of close correspondence (CC) of TSCs and axon

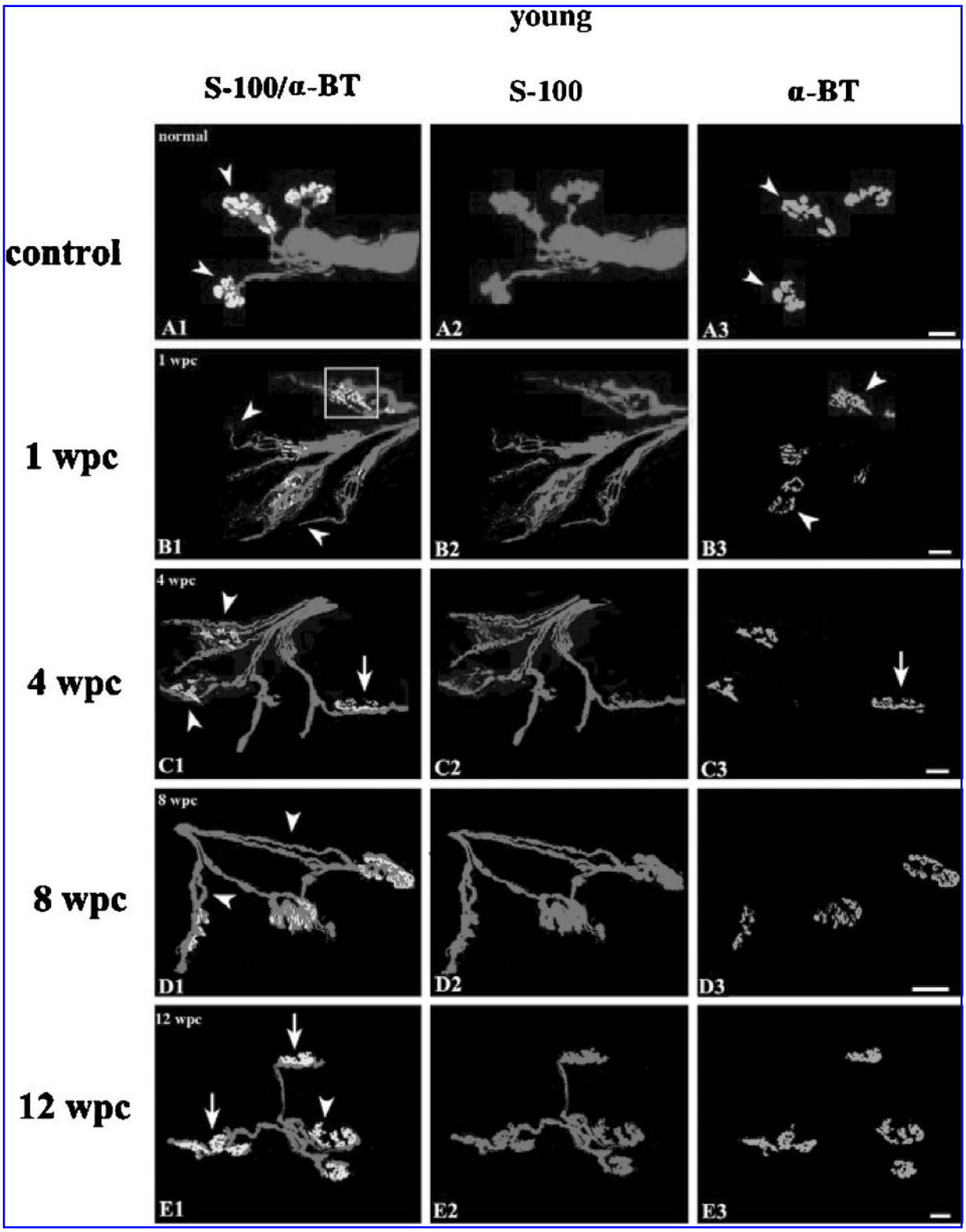

FIG. 1. Double fluorescence labeling for S-100 and 1-bungarotoxin (1-BT) was performed in longitudinal sections of soleus muscles from young unoperated control rats (**A1–A3**), and at 1 week (**B1–B3**), 4 weeks (**C1–C3**), 8 weeks (**D1–D3**), and 12 weeks post-crush (WPC; **E1–E3**). The leftmost column demonstrates the images obtained from superimposition of terminal Schwann cell (TSCs) profiles (middle column) and AChR sites (rightmost column). In unoperated rats, almost complete and exact spatial occupancy between TSCs and postsynaptic receptor regions is seen (A1, arrowheads); the ring-shaped AChR plaques are uniformly distributed (A3, arrowheads). Following injury, abundant TSC extensions (B1, B2, arrowheads) are seen at the site of the degenerating AChR sites (B3, arrowheads). At 4-WPC, single or multiple S-100–positive SC strands cross a AChR sites (C1, arrowheads). Incomplete reoccupation is shown as the greater portions of AChR plaques apposing S-100 positive TSCs (C1–C3, arrows). Arrowheads indicate multiple cell strands per NMJ (D1–D3). At 12-WPC, some NMJs show almost complete superimposition (arrows), while less developed TSCs (arrowhead) are coupled with poorly formed AChR plaques (E1–E3). Scale bar = 20 μm.

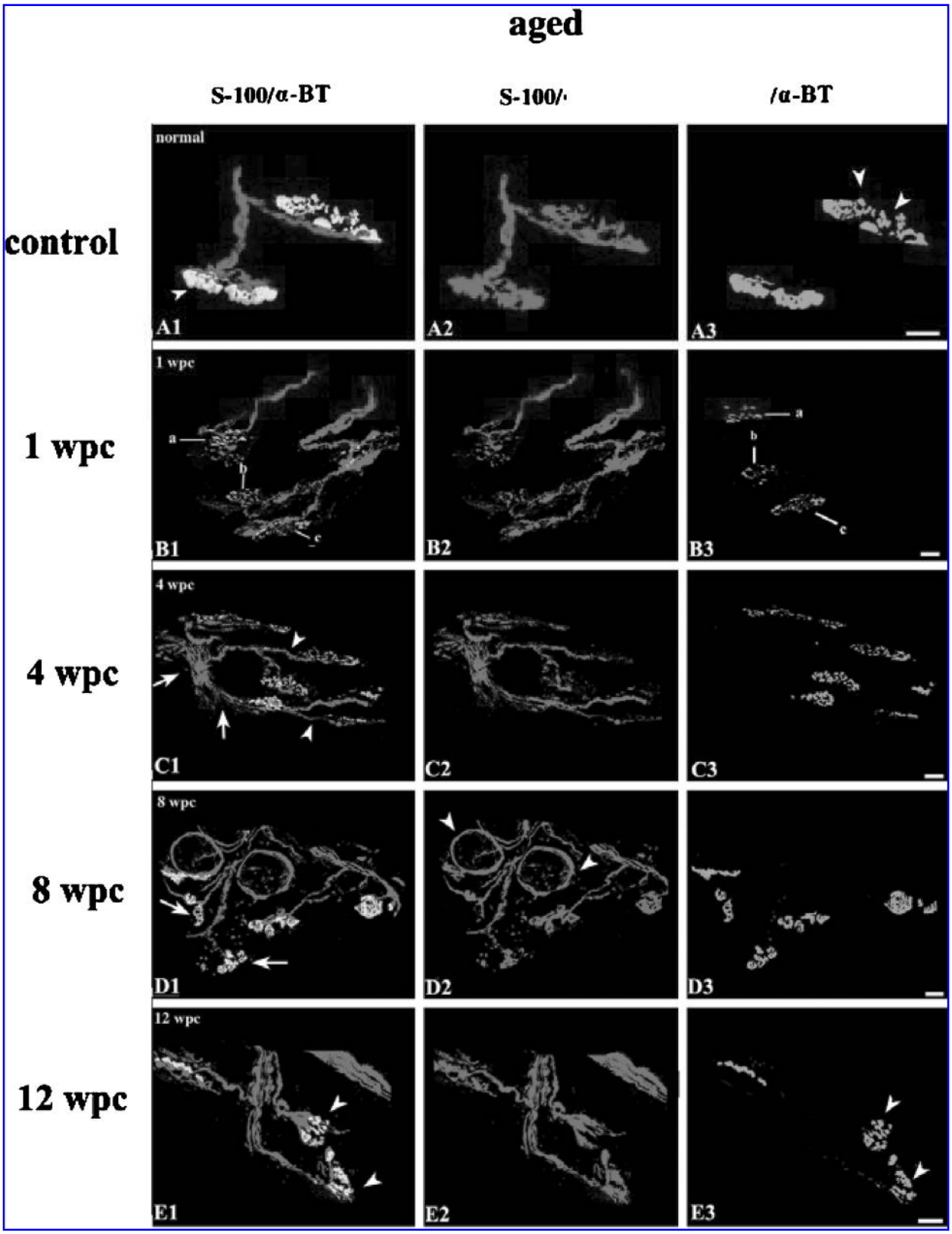

FIG. 2. Double fluorescence labeling for S-100 and 1-bungarotoxin (1-BT) in longitudinal sections of soleus muscles from aged rats. Unoperated control (**A1–A3**), 1-WPC (**B1–B3**), 4-WPC (**C1–C3**), 8-WPC (**D1–D3**), and 12-WPC (**E1–E3**). Left column, superimposed images; middle, TSCs profiles; right, AChR sites. At 1-WPC, most SCs strands exhibit irregular contours and majority of TSCs show disorganization and misalignment in NMJs (B1–3). The nerve bundles (C1, arrows) and the extensions (C1, arrowheads) from TSCs are sparse in old rats. TSCs are disintegrated in a majority of NMJs, with AChR being left unoccupied (D1, arrows). Note the loop-like debris composed of SC and AChR (D2. arrowheads). At 12-WPC, less developed TSCs are coupled with poorly formed AchR plaques (E1, E3, arrowheads). Scale bar = 20 μm.

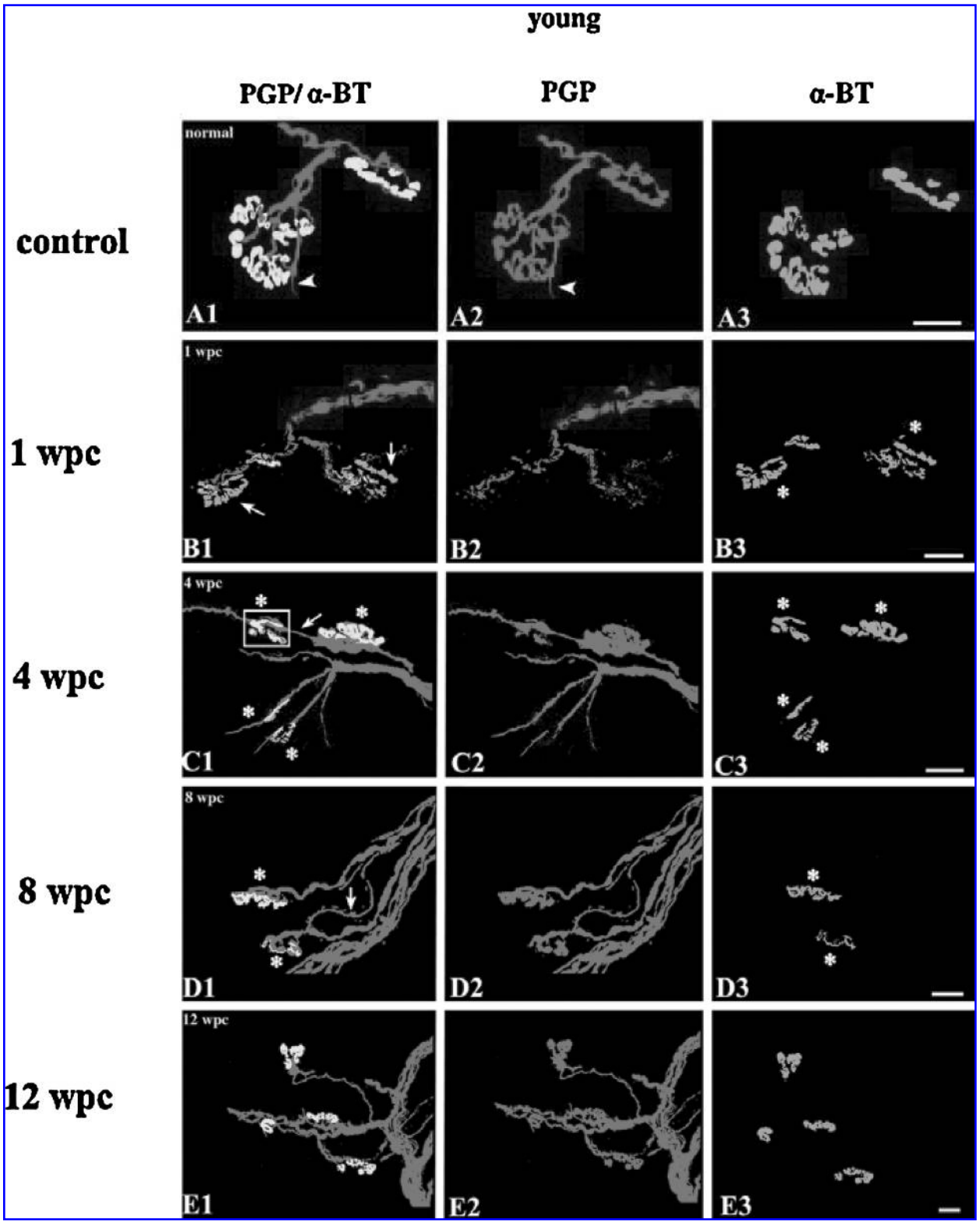

FIG. 3. Double fluorescence labeling of PGP9.5 and 1-BT from soleus muscles of young rats. **A1–A3**, unoperated control; **B1–B3**, 1-WPC; **C1–C3**, 4-WPC; **D1–D3**, 8-WPC; **E1–E3**, 12-WPC. Left column, superimposed images; middle, axon terminals; right, AChR sites. Asterisks indicate 1-BT labeling. In unoperated young rats, the superimposition between nerve terminals and postsynaptic receptor regions is nearly complete and highly accurate (A1–A3). Arrowheads in A1 and A2 indicate extraterminal sprouting. At 1-WPC, the axon terminals are disorganized and disintegrated in a majority of NMJs, with AChR plaques being left unoccupied (arrows) (B1–B3). Endplate-to-endplate sprouts (arrow) connect two junctions (C1–C3). Note immature profiles of terminals. The types of extensions contribute to multiple innervation from nodal sprouting (arrow), and the terminals are well regenerated (D1–D3). Complete reinnervation is shown by the loosely aligned thick and thin extensions clustering around the well-organized terminals at 12-WPC in young rats (E1–E3). Scale bar = 20 μm.

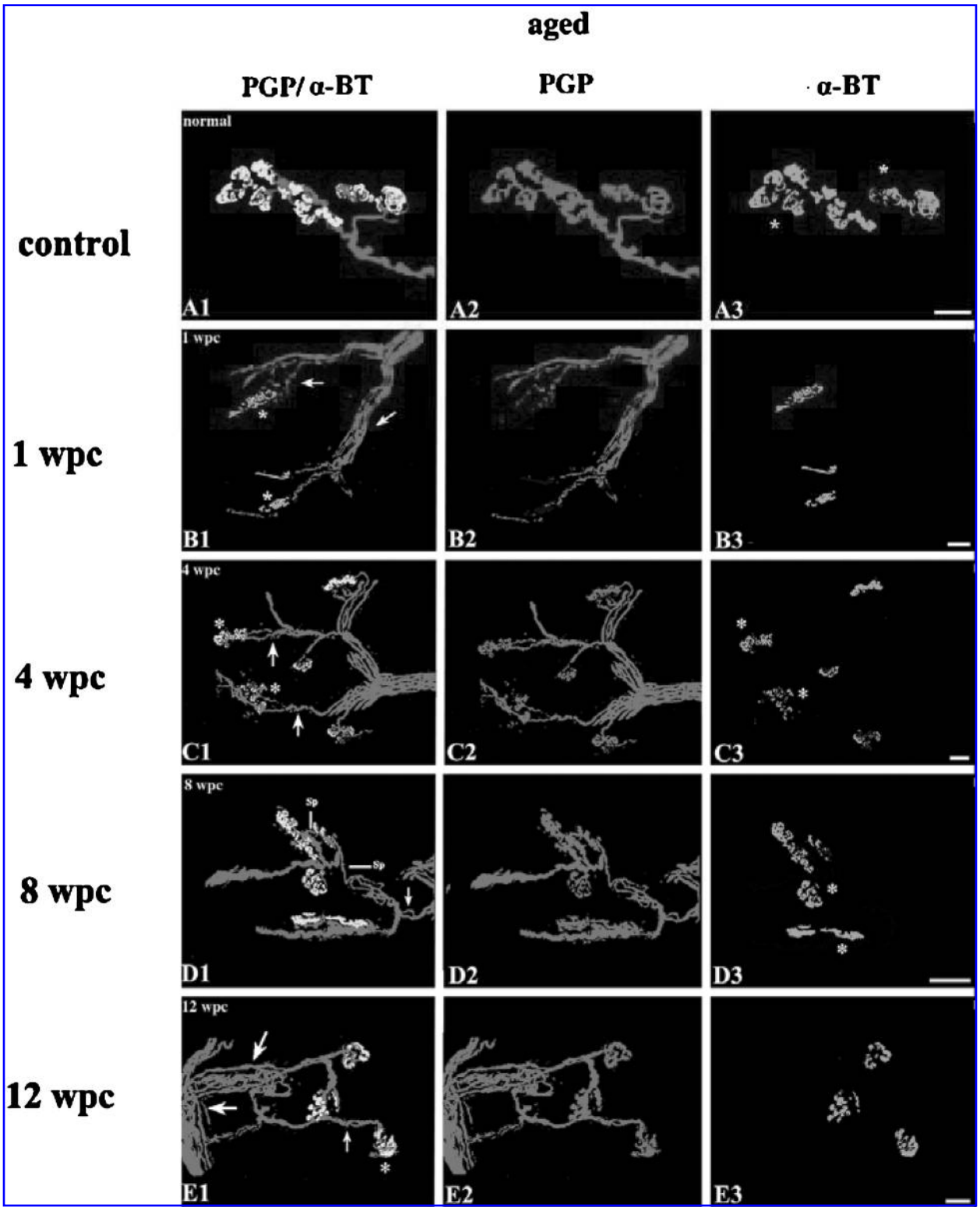

FIG. 4. Double fluorescence labeling of PGP and 1-BT from soleus muscles of old rats. **A1–A3**, unoperated control; **B1–B3**, 1-WPC; **C1–C3**, 4-WPC; **D1–D3**, 8-WPC; **E1–E3**, 12-WPC. Left column, superimposed images; middle, axon terminals; right, AchR sites. Asterisks indicate 1-BT labeling. The apposition between the nerve terminal and postsynaptic receptor is complex in the junctions of the aged rats (A1–A3). At 1-WPC, the nerve bundles were sparse (arrows) with AChR plaques being left unoccupied (asterisks; B1–B3). The pre-terminal extensions (arrows) are poorly developed. Note marked disorganization of the postsynaptic receptor regions (C1–C3). The large expanded terminal with elaborate arborizations receives a supply of two sprouts (Sp), one arising from the node of Ranvier at an adjacent nerve fiber (arrow). Shrinkage (asterisks) of the postsynaptic receptor regions is persistent (D1–D3). The endplate-to-endplate connections take a tortuous course (small arrow). Randomly aligned thick and thin extensions (large arrows) lack any determined course and uniformity in caliber and shape (E1–E3). Asterisks indicate poorly formed terminals and partially occupying an AChR. Scale bar = 20 μm.

terminals with AChR sites. About 70 junctions were evaluated at each time point. Young rats demonstrated significantly larger areas of contact between TSCs and AChR than the aged group at all post-injury time points. Similarly, by 4-WPC young rats demonstrated significantly increased contact areas of axon terminals to AChR sites compared to aged rats (Fig. 5); this increase was sustained through 12-WPC. The average numbers of axon-AChR associations in the young rats was 14 ± 2.7, and old ones 8 ± 1.5.

DISCUSSION

Three-dimensional confocal image analysis is a valuable way to assess the regeneration process in NMJs. Continuous observation of neuronal changes facilitates the location and direction of the major nerve pathways to NMJs during regeneration. To improve our understanding of the mechanism underlying nerve regeneration after injury, we reconstructed confocal images after double immunofluorescence labeling with molecular markers for regenerating axons (Hirata et al., 1997; Verdu et al., 1997) and TSCs (Trachtenberg et al., 1997; O'Malley et al., 1999; Ide et al., 1983; Ann et al., 1994). Our study demonstrates the morphological differences between the NMJs of young adult and aged rats. After injury, both SCs and nerve terminal sprouting are most active in young animals and markedly impaired in the aged ones. The most obvious difference is exemplified by persistent degeneration of SCs and axon terminals in the aged rats (data not shown). At 1-WPC, major changes include the traumatic phase of the motor axons and the reparative phase of the TSCs. At 4-WPC, the well-organized TSC strands extend into a majority of the NMJs. Most preterminals and TSCs are associated with regenerating axons. At this stage, robust process extension from TSCs is underway and the terminal axon branches approach adjacent NMJs along the TSCs processes, forming endplate-to-endplate connections. Later on, mixed nodal and extraterminal sprouting occurs. We show that in the short-term denervation, endplate-to-endplate connections, rather than nodal collateral sprouting, play a major role in reinnervation. The critical time point is 4-WPC when major morphological nerve changes convert from a degenerative to a regenerative phase.

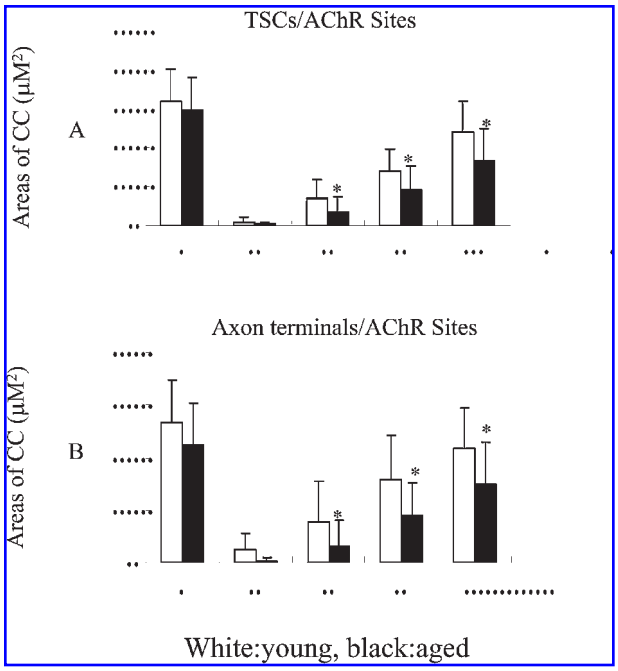

FIG. 5. Extent of close correspondence (CC) delineated by terminal Schwann cells (TSCs; **A**) or axon terminals (**B**). Values represent the mean areas ± standard error of CC among the total number of junctions. Analysis of variance (ANOVA) was used to analyze the differences between two groups at different time points. (A) The contact areas of TSCs/acetylcholine receptor (AChR) sites are lower in old rats at all time points. (B) The contact areas of axon terminals/AChR sites are lower in old rats at 4-WPC, 8-WPC, and 12-WPC.

After 4-WPC, there was a synchronous growth among the TSCs, terminal axons and AChR plaques. Regenerating TSCs and axon terminals covered large fraction of the subsynaptic membrane over the following weeks. The general shift to larger and more complex NMJs during 8–12 WPC appears to take place by elaboration of terminal branching, as well as size increases with the aid of extraterminal or nodal sprouting. Besides growing into adjacent NMJs and establishing one of the multiple synaptic contacts within or alongside the original NMJ, extraterminal sprouting contributes to increasing terminal size. The increased ability in extraterminal or nodal sprouting is then consistent with the pattern of remodeling or an adaptive mechanism for the maintenance of synaptic function as documented for adult NMJs (Cardasis et al., 1981; Wernig et al., 1986).

The complete regeneration process rate declines with age, and in old rats regeneration was delayed and recovery clearly lowered compared to the young ones. Concomitant with this, we found some specific age-related abnormalities, in the preterminal and terminal regions, such as poorly formed and damaged SCs strands and TSCs, poorly fasciculated axon bundles and poorly defined terminals as well as fine granular degeneration with frayed borders of postsynaptic AChR sites. It is likely that these abnormalities are responsible for the delay in reinnervation and regeneration in the NMJs and also a delay in the process of endplate reoccupation. On the ba-

sis of occasional degeneration changes of SCs sheaths and TSCs, it may be that some motoneurons have lost portions of their connections with the target muscles (Jacob et al., 1990b; Johnson et al., 1995). The continuing, unordered formation of regenerating axons in aged animals demonstrates varying patterns of disorder in intramuscular nerve branching. An aging-related progressive deterioration in fasciculation and branching appears to operate at the time that regenerating axons delineate their pathway within the muscle.

Two fundamental factors are proposed for the genesis of these abnormalities. Firstly, SCs are a critical factor for promoting axonal regeneration, since regenerating axons grow in the interface between SCs and their basal lamina, both of which provide substrate and trophic support (Reynolds et al., 1993). Secondly, regenerating axons usually branch at intramuscular nerve bundles, proceeding along the endomysium on the surface of denervated muscle fibers. In aged animals, the sprouted axons took a meandering path to the endplate. The regenerating axons are guided by contact-mediated mechanisms involving SCs as well as extracellular matrix (ECM) molecules (Fawett et al., 1990; Hall et al., 1993). Our study shows an increased complexity of nerve terminal arborization in the endplates of senescent rats relative to younger animals. A possible explanation is that there is an unbalanced decrease in the rates of continual growth and regression of axon terminals in the senescent rats (Scheff et al., 1979). In younger rats, the synaptic terminals of a motor axon undergo a continual process of sprouting and degeneration to maintain the endplate architecture. In the aged rats, these processes occur considerably less frequently.

Our results demonstrate the extensive processes elaborated by TSCs upon denervation and subsequent reinnervation. In young rat muscle, TSCs rapidly extend profuse networks of processes that are maintained for several weeks after injury, suggesting that the regenerating axons, on growing back to transiently denervated NMJs, use TSC processes as bridges to interconnect the motor endplates. Profuse extension of SC processes and bridge formation after peripheral nerve damage, which accompanied nerve terminal outgrowth, has been implicated in guidance of regenerating axons to denervated endplates. In young rats, TSCs produce exuberant networks of processes in early to mid-reinnervation and regeneration of NMJ, but small and short TSC processes became common progressively with time, indicating an eventual retraction and withdrawal. The poor process extension from TSCs in the early reinnervation period in aged rats may result from malformation of the TSCs in the NMJ.

On the basis of consistently high levels of close correspondence of the AChR site to TSCs or terminal axons after 4-WPC, it is evident that mechanism of close apposing between AChR sites and presynaptic elements in young adults operates from early in the reinnervation period. The sequence of changes in AChR sites over the entire interval in young adult muscle was consistent, while the proportion of reconstructed AChR plaques increases with time. In contrast, aging caused long-lasting drastic morphological abnormalities in the postsynaptic receptor region. Malformation and poor growth of the SC sheaths may affect the guidance mechanism mediated by the basal lamina tubes. The postsynaptic AChR sites within the endplate were delayed in being covered by regenerating TSCs and terminal axons in older animals. An initial drastic decline of close correspondence between AChR sites and TSCs, and between AChR sites and terminal axons appeared at 4-WPC when there was the lowest magnitude of endplate occupation. This represents a pronounced spatial misalignment, such as areas of regenerating TSCs or terminal axons that have not reoccupied the AChR site. It has been suggested that the aging-related postsynaptic abnormalities affect the degree of nerve regeneration such as muscular nerve branching as well as nerve growth at the neuromuscular synapse and the integrity of the neuromuscular contacts (Nguyen et al., 1998). Our study provide further evidence to support these previous findings.

No benefits in any form have been received or will be received from a commercial party related directly or indirectly to the subject of this article

ACKNOWLEDGMENTS

This work is supported by the Program Project Grant of the National Natural Foundation Committee (NSFC) of China (grant 30330700) and the Natural Science Foundation of Shanghai (grants 02ZB14098 and 05JC14054).

REFERENCES

ACOB, J.M., and ROBBINS, N. (1990). Age difference in morphology of reinnervation of partially denervated mouse muscle. J. Neuroosci. **10,** 1530–1540.

ANN, E.S., MIZOGUCHI, A., OKAJIMA, S., and IDE, C. (1994). Motot axin terminal regeneration as studied by protein gene product 9.5 immunohischemistry in the rat. Arch. Histol. Cytol. **57,** 317–330.

BROWN, M.C., HOLLAND, L.R., and HOPKINS, W.G. (1981). Motor nerve sprouting. Annu. Rev. Neurosci. **4,** 17–42.

CARDASIS, C.A., and PADYKULA, H.A. (1981). Ultrastructural evidence indicating reorganization at the neuromuscu-

lar junction in the normal rat soleus muscle. Anat. Rec. **200,** 41–59.

FAWETT, J.W., and KEYNES, R.J. (1990). Peripheral nerve regeneration. Ann. Rev. Neurosci. **13,** 43–46.

HALL, Z.W., and SANES, J.R. (1993). Synaptic structure and development: the neuromuscular junction. Cell. Neuronal **72,** 99–121.

HIRATA, K., ZHOU, C., NAKAMURA, K., and KAWABUCHI, M. (1997). Postnatal development of Schwann cells at neuromuscular junctions, with special reference to synapse elimination. J. Neurocytol. **26,** 799–809.

HOPKINS, W.G., LIANG, J., and BARRET, E.J. (1986). Effect of age and muscle type on regeneration of neuromuscular synapses in mice. Brain Res. **372,** 163–166.

IDE, C., TOHYAMA, K., YOKOTA, R., NITATORI, T., and ONODERA, S. (1983). Schwann cell basal lamina and nerve regeneration. Brain Res. **288,** 61–75.

JACOB, J.M., and ROBBINS, N. (1990b). Age difference in morphology of reinnervation of partially denervated mouse muscle. J. Neuroosci. **10,** 1530–1540.

JOHNSON, H.K., MOSSBERG, U., ARVIDSSON, F., PIEH, F., HOCKFELT, T., and ULFHAKE, B. (1995). Increase in a-CGRP and GAP-43 in aged motor neurons: a study of peptides, growth factors, and ChATmRNA in the lumbar spinal cord of senescent rats with symptoms of hindlimb incapacities. J. Comp. Neurol. **359,** 68–89.

LOVE, F.M., and THOMPSON, W.J. (1998). Schwann cells proliferate at rat neuromuscular junctions during development and regeneration. J. Neurosci. **15,** 9376–9385.

McMARTIN, D.N., and O'CONNOR, J.A. (1979). Effect of age on axoplasmic transport of cholinesterase in rat sciatic nerves. Mech. Ageing Dev. **10,** 241–248.

McQUARRIE, I.G., BRADY, S,T, and LASEK, R.J. (1989). Retardation in the slow axonal transport of cytosketal elements during maturation and aging. Neurobiol. Aging **10,** 359–365.

NGUYEN, Q.T., PARSADANIAN, A.S., SINDE, W.D., and LICHTMAN, J.W. (1998). Hyperinnervation of neuromuscular junctions caused by GDNF overexpression in muscle. Science **279,** 1725–1729.

O'MALLEY, J.P., WARAN, M.T., BALICE-GORDON, R.J. (1999). *In vivo* observations of terminal Schwann cells at normal, denervated, and reinnervated mouse neuromuscular junctions. J. Neurobiol. **38,** 270–286.

REYNOLDS, M.L., and WOOFLF, C.J. (1993). Reciprocal Schwann cell–axon interactions. Current Biol. **3,** 683–692.

SCHEFF, S.W., BENARDO, L.S., and COTMAN, C.W. (1979). Decrease in adrenergic axon sprouting in the senescent rat. Science **202,** 775–778.

SON, Y.J., and THOMPSON, W.J. (1995a). Schwann cell processes guide regeneration of peripheral axons. Neuron **14,** 125–132.

TANAKA, K., and WEBSTER, H.D. (1991). Myelinated fiber regeneration after crush injury is retarded in sciatic nerves of aging mice. J. Comp. Neurol. **8,** 180–187.

TRACHTENBERG, J.T., and THOMPSON, W.J. (1997). Nerve terminal withdrawal from rat neuromuscular junctions induced by neuregulin and Schwann cells. J. Neurosci. **17,** 6243–6255.

VAUGHAN, D.W. (1992). Effects of advancing age on peripheral nerve regeneration. J. Comp. Neurol. **323,** 219–237.

VERDU, E., and NAVARRO, X. (1997). Comparison of immunohistochemical and functiona; reinnervation of skin and muscle after peripheral nerve injury. Exp. Neurol. **146,** 187–198.

WERNIG, A., and HERRERA, A.A. (1986). Sprouting and remodeling at the nerve-muscle junction. Prog. Neurobiol. **27,** 251–291.

ZHOU, C.J., KAWABUCHI,M., WANG, S.Y., LIU, W.T., and HIRATA, K. (2002). Age differences in morphological patterns of axonal sprouting and multiple innervation of neuromuscular junctions during muscle reinnervation following nerve crush injury. Ann. Anat. **184,** 461–472.

Address reprint requests to:
Yong-Jun Wang, M.D.
725 Wan-Ping South Road
Institute of Spine
Shanghai University of Traditional Chinese Medicine
Shanghai-200032, China

E-mail: yjwang88@hotmail.com

This article has been cited by:

1. Dingding Shen, Qi Zhang, Xiaorong Gao, Xiaosong Gu, Fei Ding. 2011. Age-related changes in myelin morphology, electrophysiological property and myelin-associated protein expression of mouse sciatic nerves. *Neuroscience Letters* **502**:3, 162-167. [CrossRef]
2. Javier Saceda, Alberto Isla, Susana Santiago, Carmen Morales, Cristina Odene, Borja Hernández, Kenan Deniz. 2011. Effect of recombinant human growth hormone on peripheral nerve regeneration: Experimental work on the ulnar nerve of the rat. *Neuroscience Letters* . [CrossRef]
3. Núbia Broetto Cunha, Jocemar Ilha, Lígia Aline Centenaro, Gisele Agustini Lovatel, Luciane Fachin Balbinot, Matilde Achaval. 2011. The effects of treadmill training on young and mature rats after traumatic peripheral nerve lesion. *Neuroscience Letters* **501**:1, 15-19. [CrossRef]
4. Peter J. Apel, Jianjun Ma, Michael Callahan, Casey N. Northam, Timothy B. Alton, William E. Sonntag, Zhongyu Li. 2010. Effect of locally delivered IGF-1 on nerve regeneration during aging: An experimental study in rats. *Muscle & Nerve* **41**:3, 335-341. [CrossRef]
5. Peter J. Apel, Timothy Alton, Casey Northam, Jianjun Ma, Michael Callahan, William E. Sonntag, Zhongyu Li. 2009. How age impairs the response of the neuromuscular junction to nerve transection and repair: An experimental study in rats. *Journal of Orthopaedic Research* **27**:3, 385-393. [CrossRef]
6. Uroš Kovačič, Janez Sketelj, Fajko F. BajrovićChapter 26 Age-Related Differences in the Reinnervation after Peripheral Nerve Injury **87**, 465-482. [CrossRef]
7. G SHOKOUHI, R TUBBS, M SHOJA, L ROSHANGAR, M MESGARI, A GHORBANIHAGHJO, N AHMADI, F SHEIKHZADEH, J RAD. 2008. The effects of aerobic exercise training on the age-related lipid peroxidation, Schwann cell apoptosis and ultrastructural changes in the sciatic nerve of rats. *Life Sciences* . [CrossRef]

Journal of Neurotrauma 2007.24:885-894.